Kinetics of Triglyceride Solubilization by Micellar Solutions of Nonionic Surfactant and Triblock Copolymer. 2. Theoretical Model

P. A. Kralchevsky,*,† N. D. Denkov,† P. D. Todorov,† G. S. Marinov,† G. Broze,‡ and A. Mehreteab§

Laboratory of Chemical Physics & Engineering, Faculty of Chemistry, University of Sofia, 1 James Bourchier Avenue, 1164 Sofia, Bulgaria, Colgate-Palmolive R&D, Inc., Avenue du Parc Industriel, B-4041 Milmort (Herstal), Belgium, and Colgate-Palmolive Technology Center, Piscataway, New Jersey 08854-5596

Received April 15, 2002. In Final Form: July 4, 2002

A theoretical model of oil solubilization in micellar surfactant solutions is developed. We consider oils that are practically insoluble in pure water, like triolein and other triglycerides. The nonionic micelles, which are capable to solubilize such oils, are usually rodlike aggregates, composed of surfactant molecules and poly(oxyethylene)−poly(oxypropylene) triblock copolymers, like Synperonic L61 (SL61). The swollen micelles, formed after solubilization, are smaller than the empty ones. The model describes the elementary act of solubilization as a sequence of three steps: (a) adsorption of an empty micelle at the oil−water interface; (b) uptake of oil by the adsorbed empty micelle which then splits into several swollen micelles; (c) desorption of the swollen micelles. Theoretical expressions are derived, which describe the diminishing of an oil drop in the course of solubilization. The parameter values, determined from the best fit of experimental data, imply that the rate-controlling step is the step of micellar adsorption. From the determined rate constant of adsorption we estimate the respective kinetic barrier to micelle adsorption, taking into account the action of surface forces and the hydrodynamic resistance. Our analysis indicates that the triblock copolymer SL61 promotes the solubilization of triglycerides by decreasing the length of the mixed surfactant−copolymer rodlike micelles, which leads to a lowering of the kinetic barrier to their adsorption at the oil−water interface.

1. Introduction

The accumulated knowledge on kinetics of solubilization shows that there are three major solubilization mechanisms, whose effectuation depends on the specific system:[1−18]

(A) The *penetration mechanism* of Lawrence is found for some systems (mostly solid solubilizates), where the penetration of surfactant solution into the oily phase and the formation of a liquid crystalline phase at the interface is a prerequisite for the occurrence of solubilization (formation of mixed micelles).[1,2,7−9]

(B) *Direct solubilization* involves molecular dissolution and diffusion of oil into the aqueous phase with a subsequent uptake of the oil molecules by surfactant micelles.[4,12,14,18] This mechanism is operative for oils (like benzene, decane, etc.) which exhibit a sufficiently large solubility in pure water; theoretical models have been developed and verified against experiment.[12,18]

(C) *Micelle adsorption* at the oil−water interface and surface reaction is a mechanism where the central step is a direct interaction of the surfactant micelles with the interface, accompanied by a uptake of oil. This mechanism can be expected for hydrocarbons which exhibit a weak or slow solubility in pure water.[3−6,10,14−16]

The detailed kinetic mechanism of the surface reaction in case C could be multiform. Some authors[4,5] expect that the surfactant arrives at the interface in a monomeric form. Then, at the phase boundary mixed (or swollen) micellar aggregates are formed, which eventually desorb. This version of the model seems appropriate for solid solubilizates, because hemimicelles can be formed at their surfaces, even at surfactant concentrations below the bulk critical micellization concentration (cmc).[19] Another concept, presented by Plucinski and Nitsch,[10] includes a step of partial fusion of the micelles with the oil−water interface, followed by a step of separation.

* Corresponding author. Phone: (+359) 2-962 5310. Fax: (+359) 2-962 5643. E-mail: pk@lcpe.uni-sofia.bg.
† University of Sofia.
‡ Colgate-Palmolive R&D, Inc.
§ Colgate-Palmolive Technology Center.

(1) Lawrence, A.S. C. *Discuss. Faraday Soc.* **1958**, *25*, 51.
(2) Lawrence, A.S. C.; Bingham, A.; Capper, C. B.; Hume, K. *J. Phys. Chem.* **1964**, *68*, 3470.
(3) Chan, A. F.; Fennel Evans, D.; Cussler, E. L. *AIChE J.* **1976**, *22*, 1006.
(4) Carroll, B. J. *J. Colloid Interface Sci.* **1981**, *79*, 126.
(5) Huang, C.; Fennel Evans, D.; Cussler, E. L. *J. Colloid Interface Sci.* **1981**, *82*, 499.
(6) Shaeiwitz, J. A.; Chan, A. F.-C.; Cussler, E. L.; Fennel Evans, D. *J. Colloid Interface Sci.* **1981**, *84*, 47.
(7) Stowe, L. R.; Shaeiwitz, J. A. *J. Colloid Interface Sci.* **1982**, *90*, 495.
(8) Raterman, K. T.; Shaeiwitz, J. A. *J. Colloid Interface Sci.* **1984**, *98*, 394.
(9) Lim, J.-C.; Miller, C. A. *Langmuir* **1991**, *7*, 2021.
(10) Plucinski, P.; Nitsch, W. *J. Phys. Chem.* **1993**, *97*, 8983.
(11) McClements, D. J.; Dungan, S. R. *Colloids Surf., A* **1995**, *104*, 127.
(12) Kabalnov, A.; Weers, J. *Langmuir* **1996**, *12*, 3442.
(13) Coupland, J. N.; Brathwaite, D.; Fairley, P.; McClements, D. J. *J. Colloid Interface Sci.* **1997**, *190*, 71.
(14) Weiss, J.; Coupland, J. N.; Brathwaite, D.; McClements, D. J. *Colloids Surf., A* **1997**, *121*, 53.
(15) Chen, B.-H.; Miller, C. A.; Garrett, P. R. *Colloids Surf., A* **1997**, *128*, 129.
(16) Chen, B.-H.; Miller, C. A.; Garrett, P. R. *Langmuir* **1998**, *14*, 31.
(17) Weiss, J.; McClements, D. J. *Langmuir* **2000**, *16*, 5879.
(18) Todorov, P. D.; Kralchevsky, P. A.; Denkov, N. D.; Broze, G.; Mehreteab, A. *J. Colloid Interface Sci.* **2002**, *245*, 371.
(19) Somasundaran, P.; Krishnakumar, S. *Colloids Surf., A* **1997**, *123−124*, 491.

10.1021/la020366k CCC: $22.00
Published on Web 09/21/2002

The experiment[15,20] also showed that the solubilization rates for solutions of ionic surfactants are generally much smaller than those for nonionic surfactants. This can be attributed to the electrostatic repulsion between the micelles and the similarly charged surfactant adsorption monolayer at the oil−water interface.

In the present series of papers,[21,22] we investigate the kinetics of solubilization of triolein in mixed micelles of a nonionic surfactant and the triblock copolymer Synperonic L61. As nonionic surfactant we used $C_{12}E_5$ or $C_{12}E_6$ (C_{12} = dodecyl chain, E = ethylene oxide group). The light scattering experiments[21] revealed that we are dealing with large micellar aggregates, each of them containing hundreds to thousands surfactant molecules and dozens of polymer molecules. These are cylindrical aggregates of length up to 135 nm; that is, by size they resemble typical colloidal particles. Since the triolein is insoluble in water, the kinetic mechanism C is the most appropriate for interpretation of our experimental results. To achieve a quantitative comparison of theory and experiment, in this article we specify and upgrade the kinetic mechanism in the following three aspects:

(i) We assume that the empty micelles adsorb at the interface as whole aggregates, without disintegration. (ii) In conformity with the experimental findings,[21] we take into account the fact that the surface reaction of solubilization is accompanied with a splitting of the initial adsorbed aggregate to several (2−6) smaller swollen micelles. (iii) In general, we consider a mixed barrier−diffusion control of the solubilization process. The resulting model contains several kinetic parameters: rate constants of micelle adsorption, reaction, and desorption and micelle diffusion coefficients. The comparison with experimental data indicates which of the steps is rate-controlling. One of our major aims is to understand how the triblock copolymer SL61 promotes the solubilization.

The paper is organized as follows. In section 2 we summarize the basic experimental facts. Section 3 exposes the model itself. In section 4 we estimate the geometric correction factor, which accounts for the fact that in our experiments the oil drops are located below a glass plate rather than in the bulk of the micellar solution. Section 5 is devoted to derivation of an expression for the adsorption rate constant and to an estimate for the kinetic barrier to micelle adsorption from the experimental value of the rate constant. In the third part of this series[22] we apply the developed model to interpret results from a systematic series of experiments on triolein solubilization.

2. Background and Preliminary Experiments

As reported in part 1 of this series,[21] and as known from previous studies,[4,15] the solubilization ability of *nonionic* surfactants (such as $C_{12}E_5$ and $C_{12}E_6$) increases when the temperature of the system approaches the cloud point from below. The latter can be achieved in two ways: by increase of the temperature of solution; by decrease of the cloud-point temperature with the help of added inorganic salts, such as Na_2SO_4.[23] Both ways have the same consequences: (i) growth of large elongated micelles; (ii) conversion of the micelle−micelle (and micelle−oil drop) interaction from repulsive to attractive. The latter two effects have the same physical origin: increasingly attractive force between the ethoxy groups in the surfactant adsorption monolayers.[24,25]

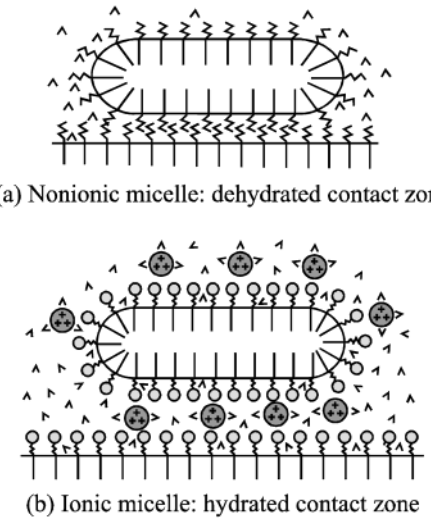

Figure 1. Rodlike micelle adsorbed at an oil−water interface covered with a surfactant monolayer. (a) Nonionic surfactant close to the cloud point; due to the ethoxy-chain dehydration, the contact zone micelle−interface is partially hydrophobic. (b) Anionic surfactant in the presence of Al^{3+} counterions; surfactant headgroups and counterions are both well hydrated, which creates a water-rich contact zone.

The aforementioned micellar transformations can be easily related to the detected enhancement of triglyceride solubilization,[21,22] if one assumes that the adsorption (transient attachment) of micelles at the oil−water interface is a necessary step in the process of solubilization (Figure 1a). Indeed, the micelle−oil drop attraction is a prerequisite for the micelle adsorption. The greater length of the nonionic micelles can lead to a larger contact area and stronger micelle-to-interface adhesion.

Large rodlike micelles can be formed also in solutions of *anionic* surfactants in the presence of inorganic electrolytes and especially of salts with divalent and trivalent counterions.[26,27] To check whether such micelles are able to solubilize triglycerides, we carried out experiments on solubilization of triolein in solutions of sodium dodecyl dioxyethylene sulfate (SDP2S) in the presence of Al^{3+} counterions. In ref 27 it has been shown that the binding of Al^{3+} to the SDP2S headgroups essentially reduces the micelle negative surface charge and gives rise to the formation of long rodlike micelles. Moreover, one could hypothesize that the Al^{3+} ions might bridge between the micelle and the oil−water interface and bring about micelle adsorption (Figure 1b). However, our experiments with the system SDP2S + Al^{3+} showed that triolein is not solubilized in such anionic micellar solutions. The reasons for this negative result could be at least two: (i) Despite the binding of Al^{3+}, the surface charge remains large enough to prevent the micelle adsorption at the oil−water interface. (ii) Even if micellar adsorption takes place (Figure 1b), the water-rich film, intervening between

(20) Ward, A. J. I. In *Solubilization in Surfactant Aggregates*; Christian, S. D., Scamehorn, J. F., Eds.; M. Dekker: New York, 1995; Chapter 7.

(21) Christov, N. C.; Denkov, N. D.; Kralchevsky, P. A.; Broze, G.; Mehreteab, A. *Langmuir* **2002,** *18*, 7880.

(22) Todorov, P. D.; Marinov, G. S.; Kralchevsky, P. A.; Denkov, N. D.; Broze, G.; Mehreteab, A. *Langmuir* **2002,** *18*, 7896.

(23) Broze, G. In *Solubilization in Surfactant Aggregates*; Christian, S. D., Scamehorn, J. F., Eds.; M. Dekker: New York, 1995; Chapter 15.

(24) Claesson, P. M.; Kjellander, R.; Stenius, P.; Christenson, H. K. *J. Chem. Soc., Faraday Trans. 1* **1986**, *82*, 2735.

(25) Israelachvili, J. N. *Intermolecular and Surface Forces*; Academic Press: London, 1992.

(26) Alargova, R. G.; Ivanova, V. P.; Kralchevsky, P. A.; Mehreteab, A.; Broze, G. *Colloids Surf., A* **1998**, *142*, 201.

(27) Alargova, R. G.; Danov, K. D.; Kralchevsky, P. A.; Broze, G.; Mehreteab, A. *Langmuir* **1998**, *14*, 4036.

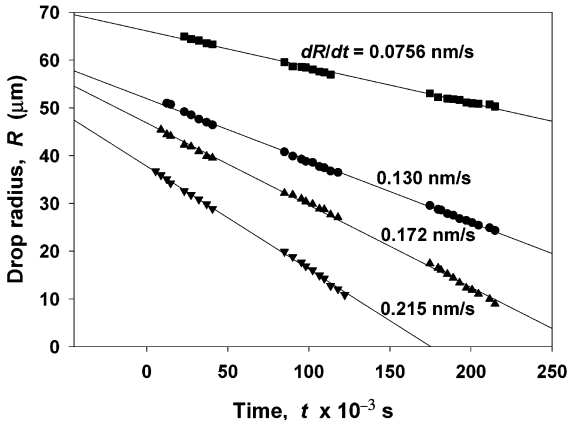

Figure 2. Solubilization of triolein drops in a solution of 12 mM $C_{12}E_5$ + 0.01 M NaCl at 27 °C, with added 0.1 wt % Synperonic L61: Experimental dependence of the drop radius R on time, t.

micelle and oil, may create a high kinetic barrier to the transfer of hydrophobic triglyceride molecules from the oil phase into the micelle.

The described results about the occurrence or lack of triglyceride solubilization in nonionic/anionic surfactant solutions imply that the accomplishment of optimal conditions for solubilization is a matter of tuning of two oppositely directed trends: (i) Partial *hydrophobization* of the surfactant headgroups which would allow micelle adsorption and transfer of triglyceride molecules from the oil phase into the micelle. (ii) Preserving the *amphiphilic* nature of the surfactant which should be soluble in water (rather than in oil) and able to adsorb and form micelles. Examples for such tuning are described in part 3 of this study,[22] where it is shown that the addition of small amounts of the anionic surfactant SDP2S to the nonionic $C_{12}E_6$ leads to deceleration and complete ceasing of triglyceride solubilization (due to the increased electrostatic repulsion between the micelle and interface). Subsequent addition of the amphoteric surfactant alkyldimethylamine oxide (AO) to the solution restores and accelerates the solubilization.[22] AO is known to form electroneutral complexes with SDP2S,[28] which means that we encounter another example for enhancement of triglyceride solubilization by suppressing the repulsion between the micelles and the oil−water interface.

In the next section we propose a kinetic model of triglyceride solubilization, which is based on the aforementioned experimental facts. An additional fact, which has to be explained by the model, stems from the finding that the rate of solubilization of oil drops depends on their initial size. As an example, in Figure 2 we show the experimental dependencies for 4 separate triolein drops in solutions of 12 mM $C_{12}E_5$ + 0.1 wt % SL61 + 0.01 M NaCl. Each drop is injected in a horizontal capillary filled with the investigated solution, and the diminishing of its radius, R, is observed microscopically and recorded as a function of time t (experimental details in ref 22). For each separate drop, the dependence $R(t)$ is approximately a straight line, whose slope increases with the decrease of the initial drop size. In other words, the solubilization is faster for the smaller drops. The kinetic data in Figure 2 are not consistent with a regime of simple diffusion control, which predicts dR^2/dt = constant.

(28) Oldenhove de Guertechin, L. In *Handbook of Detergents, Part A: Properties*, Broze, G., Ed.; M. Dekker: New York, 1999; Chapter 2.

3. Theoretical Model of Triglyceride Solubilization

3.1. Basic Assumptions and Equations. First, we note that the model presented below is applicable to any oil (not necessarily a triglyceride) which exhibits a negligible molecular solubility in pure water. On the basis of the discussion in section 2 and our previous results,[21] we assume that the elementary act of solubilization includes the following three consecutive steps (Figure 3):

(a) *adsorption* of an empty surfactant micelle at the oil−water interface;

(b) *uptake of oil*, accomplished by the surface reaction

$$\{\text{empty micelle}\} + \{\text{oil molecules}\} = m\{\text{swollen micelles}\} \quad (3.1)$$

(c) *desorption* of the swollen micelles.

Equation 3.1 takes into account the experimental fact that the long cylindrical empty micelles split into m smaller aggregates (cylindrical or spherical) in the course of solubilization. Note that the micelles (empty and swollen) are not monodisperse in size, so that m is an average value. In particular, m takes values from 1.8 to 5.4 for the micellar solutions investigated in the first part of this study.[21] According to Granek,[29] the breakup of cylindrical micelles upon swelling with oil can be attributed to a spontaneous curvature-induced Rayleigh-like instability.

In the framework of the Langmuir model of adsorption, we have

$$\theta_0 + m\frac{\Gamma_1}{\Gamma_\infty} + \frac{\Gamma_2}{\Gamma_\infty} = 1 \quad (3.2)$$

Here and hereafter index 1 denotes empty micelles and index 2 denotes swollen micelles, Γ_1 and Γ_2 are the respective adsorptions of micelles at the oil−water interface (number of micelles/unit area), θ_0 is the area fraction of the empty adsorption sites, and Γ_2/Γ_∞ and $m\Gamma_1/\Gamma_\infty$ are respectively the area fractions occupied by swollen and empty micelles. We have taken into account that an empty micelle occupies m times greater area than a swollen micelle; Γ_∞^{-1} is the area/adsorption site. The net adsorption fluxes of empty and swollen micelles (number of micelles adsorbing/unit area and unit time) are[30]

$$Q_1 = k_{1,a}c_{1s}\theta_0^{\,m} - k_{1,d}\Gamma_1 \quad (3.3)$$

$$Q_2 = k_{2,a}c_{2s}\theta_0 - k_{2,d}\Gamma_2 \quad (3.4)$$

Here $k_{i,a}$ and $k_{i,d}$ are the kinetic constants of adsorption and desorption of empty ($i = 1$) and swollen ($i = 2$) micelles, $c_{is} \equiv c_i(r = R)$, $i = 1$ and 2, by definition are the "subsurface" concentrations of the empty and swollen micelles, where $c_i(r)$, $r \geq R$, is the radial dependence of the concentration of the respective diffusing micelles in the aqueous phase around a spherical oil drop of radius R, and the coordinate origin, $r = 0$, is fixed at the drop center. In general, c_{1s} and c_{2s} differ from the respective bulk micelle concentrations, c_{10} and c_{20}, due to the diffusion and the surface solubilization reaction; see eq 3.8. The surface

(29) Granek, R. *Langmuir* **1996**, *12*, 5022.

(30) Benson, S. W. *The Foundations of Chemical Kinetics*; McGraw-Hill: New York, 1960.

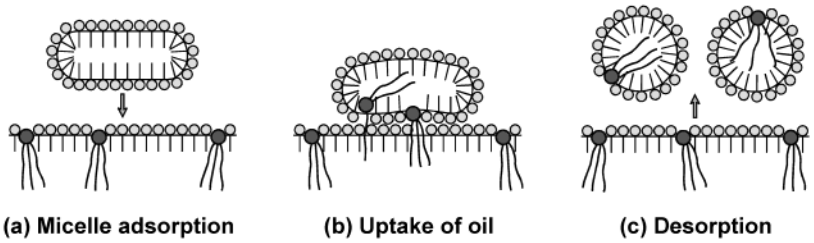

Figure 3. Elementary act of solubilization modeled as a sequence of three steps: (a) adsorption of an empty micelle at the oil−water interface; (b) uptake of oil accomplished as a surface reaction, where the empty micelle takes oil and splits into several swollen micelles; (c) desorption of the swollen micelles. In our experiments the oil is a triglyceride, which is depicted schematically as a molecule with three tails.

mass balances of empty and swollen micelles can be expressed in the form

$$\frac{d\Gamma_1}{dt} = -k_s\Gamma_1 + Q_1 \quad \frac{d\Gamma_2}{dt} = mk_s\Gamma_1 + Q_2 \qquad (3.5)$$

where k_s is the rate constant of solubilization, i.e., of the surface reaction described by eq 3.1. Equation 3.5 presumes that the solubilization is an *irreversible* process. In a *stationary* regime ($d\Gamma_i/dt = 0$), eq 3.5 yields

$$Q_1 = k_s\Gamma_1 \quad Q_2 = -mk_s\Gamma_1 \quad Q_2 = -mQ_1 \qquad (3.6)$$

Next, let us consider a spherical oil drop of radius R. In a stationary regime, the diffusional transport of empty and swollen micelles toward the drop surface is described by the equation

$$c_i(r) = c_{i0} - \frac{Q_1R^2}{D_ir} \qquad i = 1, 2 \qquad (3.7)$$

where D_i is the micelle diffusion coefficient. Equation 3.7 is the solution of the stationary diffusion equation $(d/dr)(r^2(dc_i/dr)) = 0$, satisfying the boundary conditions $c_i(r \to \infty) = c_{i0}$ and $D_i(\partial c_i/\partial r)_{r=R} = Q_i$. Then, the subsurface concentrations of the empty and swollen micelles are

$$c_{is} = c_i|_{r=R} = c_{i0} - \frac{R}{D_i}Q_i \qquad i = 1, 2 \qquad (3.8)$$

Equations 3.2−3.5 and 3.8 form a system of 7 equations for determining the 7 unknown variables Q_1, Q_2, Γ_1, Γ_2, c_{1s}, c_{2s}, and θ_0. In particular, this system of equations determines the dependence $Q_1 = Q_1(R)$.

The decrease of the oil-drop volume, V, with time, t, during solubilization can be expressed in the form

$$-\frac{dV}{dt} = v_1\lambda(4\pi R^2)(-Q_2) \qquad (3.9)$$

where v_1 is the volume of oil taken by one swollen micelle and λ is a geometrical correction factor that accounts for the fact that in our experiments the oil drop is situated in the vicinity of a glass surface rather than in the bulk of the aqueous phase.[22] In section 4 we show that one can set $\lambda = 0.9$ for a spherical drop located below a flat plate. Substituting $Q_2 = -mQ_1$ and $V = (4/3)\pi R^3$ in eq 3.9, we obtain a differential equation for $R(t)$:

$$\frac{dR}{dt} = -\lambda m v_1 Q_1(R) \qquad (3.10)$$

In principle, eq 3.10, with $Q_1(R)$ determined from eqs 3.2−3.5 and 3.8, enables one to interpret theoretically the experimental dependence $R(t)$. Below we consider the simpler (but physically important) case of solubilization in the Henry regime, in which the set of equations can be linearized and the expression for $R(t)$ can be obtained in a convenient explicit form.

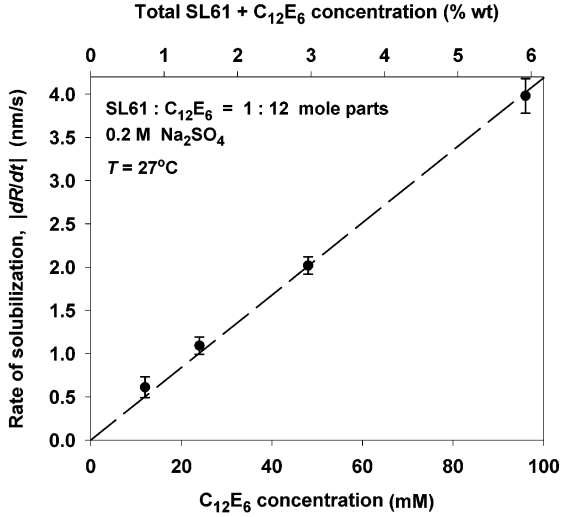

Figure 4. Rate of solubilization of soybean oil drops, dR/dt, vs the total concentration of $C_{12}E_6$. All solutions contain Synperonic L61 in molar ratio SL61: $C_{12}E_6$ = 1:12. The background electrolyte is 0.2 M Na_2SO_4; the temperature is T = 27 °C.

3.2. Solubilization of Triglycerides in the Henry Regime. The experiment shows that for the systems investigated in refs 21 and 22 ($C_{12}E_n$ + SL61) the rate of solubilization grows almost linearly with the increase of the micelle concentration. For example, Figure 4 shows data about the solubilization of soybean oil by EO6 + SL61 + 0.2 M Na_2SO_4, characterized by the rate of decrease of the radius of an oil drop, $|dR/dt|$ (initial drop radius $R_0 \approx 40\ \mu$m). Analogous linear dependence is obtained for the other investigated system, EO5 + SL61 + 0.01 M NaCl. In the studied concentration range, the experimental curves do not exhibit a tendency for saturation (leveling off) at the higher surfactant concentrations. This indicates the occurrence of micelle adsorption in Henry regime. In other words, the occupancy of the oil−water interface with adsorbed micelles is relatively low. Hence, in view of eq 3.2, we obtain

$$m\frac{\Gamma_1}{\Gamma_\infty} + \frac{\Gamma_2}{\Gamma_\infty} \ll 1 \quad \theta_0 \approx 1 \qquad (3.11)$$

Setting $\theta_0 \approx 1$ in eqs 3.3 and 3.4 and using eq 3.6, we obtain a set of two linear equations for Γ_1 and Γ_2, whose solution reads

$$\Gamma_1 = \frac{k_{1,a}}{k_s + k_{1,d}}c_{1s} \quad \Gamma_2 = \frac{k_{2,a}}{k_{2,d}}c_{2s} + \frac{mk_sk_{1,a}}{k_s + k_{1,d}}c_{1s} \qquad (3.12)$$

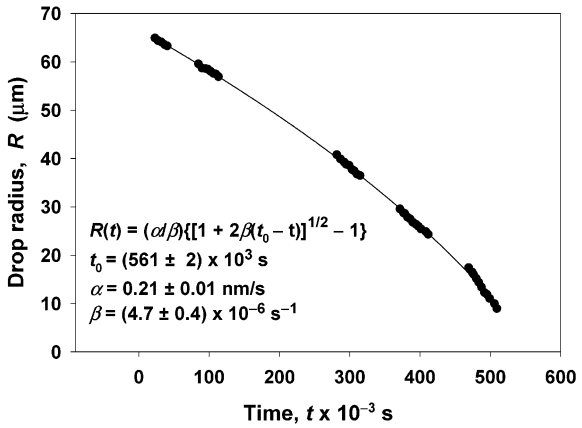

Figure 5. Data from Figure 2 (triolein drops in a solution of 12 mM $C_{12}E_5$ + 0.01 M NaCl at 27 °C, with 0.1 wt % Synperonic L61) processed with the help of eq 3.18. The continuous line is the best fit; see the text for details.

Next, combining eqs 3.6 and 3.12, we obtain an expression for the stationary adsorption flux of empty micelles:

$$Q_1 = k_s\Gamma_1 = \chi c_{1s} \quad \chi \equiv \frac{k_s k_{1,a}}{k_s + k_{1,d}} \tag{3.13}$$

χ has the meaning of a compound rate constant of solubilization. Furthermore, eliminating c_{1s} between eqs 3.8 and 3.13, we get the explicit dependence $Q_1(R)$:

$$Q_1 = \frac{\chi c_{10}}{1 + \chi R/D_1} \tag{3.14}$$

Finally, we substitute eq 3.14 into eq 3.10 and bring the result in the form

$$\frac{dR}{dt} = -\frac{\alpha}{1 + (\beta/\alpha)R} \tag{3.15}$$

where

$$\alpha = \lambda m v_1 \chi c_{10} \tag{3.16}$$

$$\beta = \lambda m v_1 \chi^2 c_{10}/D_1 = \frac{\alpha^2}{\lambda m v_1 c_{10} D_1} \tag{3.17}$$

The integration of eq 3.15 yields

$$R(t) = \frac{\alpha}{\beta}\{[1 + 2\beta(t_0 - t)]^{1/2} - 1\} \qquad t \le t_0 \tag{3.18}$$

In eq 3.18 we have determined the integration constant from the boundary condition

$$R(t_0) = 0 \tag{3.19}$$

where t_0 is the moment of disappearance of the diminishing oil drop in the actual experiment (see Figure 5). The square-root time dependence, $R(t)$, in eq 3.18 resembles the law of diminishing of a liquid drop upon molecular dissolution into another liquid (e.g. benzene in water), although the functional form and the parameters meaning are somewhat different; see e.g. eq 23 in ref 18.

By fitting the experimental data for $R(t)$ with the help of eq 3.18, one can determine the parameters α and β. Next, from the values of α and β one can calculate the average number of oil molecules solubilized in a swollen micelle, n_s, and the kinetic parameter χ:

$$n_s \equiv \frac{v_1}{v_o} = \frac{1}{\lambda m c_{10} D_1 v_o}\frac{\alpha^2}{\beta} \qquad \chi = \frac{\beta}{\alpha} D_1 \tag{3.20}$$

Here v_o denotes the volume of an oil molecule. Note that $c_{10} = (c_s - \text{cmc})/N_{\text{surfact.}}$, where c_s is the total surfactant concentration and $N_{\text{surfact.}}$ is the number of surfactant molecules/empty micelle, as given in ref 21, Table 1.

3.3. Discussion. If the uptake of oil in the adsorbed micelles is much faster than their desorption, then $k_s \gg k_{1,d}$ and eq 3.13 yields

$$\chi \approx k_{1,a} \quad k_s \gg k_{1,d} \tag{3.21}$$

In this limiting case, the micelles are expected to take the maximum possible amount of oil; in other words, we are dealing with micelles which are equilibrated with the oil phase. Then, n_s is expected to be equal to the equilibrium value of N_{triolein} given in Table 1 of ref 21—the data for 10 days equilibration. Hence, the comparison of the independently measured values of n_s and N_{triolein}(equilibrium) provides an opportunity to verify the kinetic model; see ref 22.

Note that if the condition $k_s \gg k_{1,d}$ is not satisfied, the adsorbed micelles may desorb before the saturation of their solubilization capacity, i.e., before their equilibration with the oil phase. For such "partially swollen" micelles one has $n_s < N_{\text{triolein}}$.

Since α and β are independent of R, eq 3.15 predicts that the rate of solubilization, $|dR/dt|$ should increase with the decrease of the drop radius R. This prediction is consonant with the experimental data in Figure 2. The lines in Figure 2 could be regarded as small portions of the theoretical curve $R(t)$ given by eq 3.18. In other words, owing to the stationary regime of the process, the lines in Figure 2 (from the upper toward the lower one) can be considered as consecutive stages of diminishing of the same drop but recorded with respect to different initial moments $t = 0$. To check this conjecture, we assembled a single curve from the lines in Figure 2 by means of the following procedure. The upper line is fixed; the next lower line is translated horizontally, to the right, until its left-hand side point lies on the upper line. This is repeated with the subsequent two lower lines. The resulting "compound" line is shown in Figure 5, where the continuous curve is the best fit drawn by means of eq 3.18. (An alternative but equivalent procedure for data processing, which avoids shifting of the experimental curves, is described in the Appendix to part 3 of this series.[22]) The parameter values determined from the best fit are

$$\alpha = 0.21 \pm 0.01 \text{ nm/s} \quad \beta = (4.7 \pm 0.4) \times 10^{-6} \text{ s}^{-1}$$
$$t_0 = (561 \pm 2) \times 10^3 \text{ s} \tag{3.22}$$

Substituting the latter values of α and β in eq 3.20, along with parameter values $\lambda = 0.9$ (see section 4), $m = 5.4$, $c_{10} = 3.9 \times 10^{15}$ cm^{-3}, $D_1 = 1.5 \times 10^{-7}$ cm^2/s (from ref 21), and $v_o = 1.63$ nm^3, we calculate that the number of triolein molecules taken by one swollen micelle is $n_s \approx 20$. In fact, the latter value coincides with the value $N_{\text{triolein}} = 20 \pm 3$ of the oil molecules contained in an average swollen micelle after preequilibration (for 10 days) with triolein, as independently determined by NMR in ref 21. This encouraging agreement, and the good fit of the data in Figure 5 (and many similar sets of data in ref 22), show that (i) the proposed kinetic model is applicable to the investigated experimental system and (ii) in this system the surface reaction, eq 3.1, takes less time than the average duration of a micelle stay at the interface (in

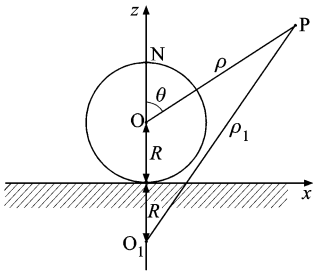

Figure 6. Sketch of a spherical oil drop in contact with a solid surface. ρ and ρ_1 are the distances from a point P to the center of the sphere, O, and its mirror image, O_1, respectively.

adsorbed state), that is, eq 3.21 holds. In such a case, by substituting the above values of α, β, and D_1 in eq 3.20, we determine the kinetic constant of adsorption of empty micelles:

$$k_{1,a} \approx \chi = 336 \text{ nm/s} \tag{3.23}$$

In section 5 we discuss whether the latter value of $k_{1,a}$ is reasonable.

The procedure of assembly of the "compound" curve in Figure 5 from the separate lines in Figure 2 might seem imperfect. Indeed, it is more convincing to carry out a *long-time* experiment with a single diminishing drop rather than to assemble a "compound" curve from the data for several *short-time* experiments with different drops. The results from such long-time experiments are reported in the next part of this study.[22] The obtained values for n_s from the "long"- and "short"-time experiments coincide within 10%, which is an argument in favor of the proposed model.

4. Calculation of the Geometric Correction Factor

As already mentioned, in our experiments[22] the oil drop, which is immersed in a micellar surfactant solution, is located below a glass surface due to the action of the buoyancy force. The microscopic observations show that the drops ($R \leq 50\ \mu$m) are spherical and that they do not stick to the glass wall; this indicates the presence of an aqueous film separating the drops from the glass. Our goal here is to estimate the deceleration of the diminishing of an oil drop located in the vicinity of a solid wall (Figure 6), in comparison with a similar drop situated in the bulk of solution. The *xy*-plane of the coordinate system coincides with the solid surface, while the *z*-axis is chosen to pass through the center of the spherical drop. We seek a solution, $c(x,y,z)$, of the equation of stationary diffusion,

$$\nabla^2 c = 0 \tag{4.1}$$

satisfying the boundary condition

$$(\partial c/\partial z)_{z=0} = 0 \tag{4.2}$$

Equation 4.2 means that the diffusion flux across the plane $z = 0$ (the solid surface) is zero. The latter restriction on the diffusion flux is the reason for some deceleration of the drop dissolution. For brevity, here and hereafter we skip the subscripts "1" and "2" of quantities such as c, D, etc. One can check that the solution of the boundary problem (4.1) and (4.2) is

$$c = A\left(\frac{1}{\rho} + \frac{1}{\rho_1}\right) \tag{4.3}$$

where A is a constant of integration and

$$\rho = [x^2 + y^2 + (z - R)^2]^{1/2} \quad \rho_1 = [x^2 + y^2 + (z + R)^2]^{1/2} \tag{4.4}$$

ρ and ρ_1 represent the distances from the point P, where the concentration c is evaluated, to the center of the sphere, O, and to its mirror image O_1, respectively; see Figure 6. Let us introduce polar coordinates (r,θ,φ) with origin at the center of the spherical drop, point O. In terms of the polar coordinates, eq 4.4 acquires the form

$$\rho = r \quad \rho_1 = (r^2 + 4Rr\cos\theta + 4R^2)^{1/2} \tag{4.5}$$

To estimate the constant A, we assume that the flux at the upper point of the drop, point N in Figure 6, is the same as for a drop of the same radius in the bulk:

$$-D\left.\frac{\partial c}{\partial r}\right|_{r=R;\theta=0} = Q \tag{4.6}$$

Substituting eq 4.3 into eq 4.6, we determine the integration constant:

$$A = 0.9QR^2/D \tag{4.7}$$

The flux of oil molecules per unit area of the drop surface (Figure 6) can be expressed in the form

$$\tilde{Q}(\theta) = -D\left.\frac{\partial c}{\partial r}\right|_{r=R} = AD\left(\frac{1}{R^2} + \frac{1}{\rho_1^2}\frac{\partial \rho_1}{\partial r}\right)_{r=R} \tag{4.8}$$

where $\rho_1 = \rho_1(r,\theta)$; see eq 4.5. The average value of the flux is

$$\bar{Q} = \frac{1}{4\pi R^2}\int_0^{2\pi} d\varphi \int_0^{\pi} d\theta R^2 \sin\theta\, \tilde{Q}(\theta) \tag{4.9}$$

Furthermore, we substitute eq 4.8 into eq 4.9. The integration can be carried out analytically with the help of the following auxiliary relationship:

$$\left.\frac{\partial \rho_1}{\partial r}\right|_{r=R} = \left(\frac{1}{2R} + \frac{\cos\theta}{R}\right)\left.\frac{\partial \rho_1}{\partial(\cos\theta)}\right|_{r=R} \tag{4.10}$$

One can check that the integration of eq 4.9 yields

$$\bar{Q} = \lambda Q \quad \lambda = 0.9 \tag{4.11}$$

The latter value, $\lambda = 0.9$, is to be substituted in the expressions in section 3, if the geometry of the experimental system corresponds to that depicted in Figure 6. The value $\lambda = 0.9$ was confirmed by independent experiments on molecular dissolution of benzene drops in water for surfactant concentrations below the cmc. For the diffusion in the latter system the same consideration is applicable; the theory was found to fit excellently the data without using any adjustable parameters.[18]

5. Rate Constant of Micelle Adsorption

5.1. Expression for the Rate Constant. The experimental results, reported in the other two parts of this study,[21,22] indicate that the added copolymer SL61 accelerates the process of solubilization without changing the equilibrium solubilization capacity of the surfactant solution. In other words, SL61 acts like a catalyst which lowers the activation energy of the process. This issue

deserves a closer examination to understand better how the copolymer affects the solubilization (by decrease of the micelle size, by enhancing the attractive forces, etc.).

From the viewpoint of the kinetic theory, $k_{1,a}$ is related to the height of the barrier to micelle adsorption

$$k_{1,a} = P \exp\left(-\frac{E_a}{kT}\right) \tag{5.1}$$

where E_a is the respective activation energy (height of the barrier), k is the Boltzmann constant, T is the temperature, and P is a preexponential factor. To determine P we have to undertake some model considerations. For simplicity, let us assume that the rodlike empty micelles approach the oil−water interface as depicted in Figure 3a, that is with their long axes parallel to the phase boundary. In such a case, $k_{1,a}$ can be expressed in the form

$$k_{1,a} = kT\,[\int_0^\infty \mu(h)\mathrm{e}^{U(h)/kT}\,\mathrm{d}h]^{-1} \tag{5.2}$$

where h is the surface-to-surface distance between a micelle and the oil water interface, $U(h)$ is the respective interaction energy due to the surface forces, and $\mu(h)$ is the hydrodynamic resistance related to the energy dissipation, which accompanies the outflow of a viscous liquid from the narrow gap between the micelle and the interface. To obtain eq 5.2 we followed the standard approach of Fuchs[31] described in the book by Derjaguin,[32] with the only difference that the geometry is "cylinder−plane" (Figure 3a) rather than "sphere−sphere".

We will model the micelles as cylinders of radius a and length $L = 2b$. For the empty micelles, investigated in ref 21, it has been established that $9.3 \le b/a \le 24$. When such cylinder is approaching a flat surface, which is parallel to the cylinder axis, the hydrodynamic resistance is given by the expression[33]

$$\mu(h) = 3\sqrt{2}\pi\eta(a/h)^{3/2}L \tag{5.3}$$

where η is the viscosity of the liquid medium.

The interaction energy $U(h)$ is expected to have a maximum, which is to be identified as the kinetic barrier to micelle adsorption:[32]

$$E_a = U_{max} \quad h = h_m \tag{5.4}$$

Following Derjaguin,[32] we use the latter fact to evaluate the integral in eq 5.2 by the steepest descent method. Thus, using eq 5.3, we bring eq 5.2 in the form

$$k_{1,a} \approx \frac{[kT(-U''_m)]^{1/2}}{6\eta L}\left(\frac{h_m}{\pi a}\right)^{3/2}\exp\left(-\frac{E_a}{kT}\right) \tag{5.5}$$

Cf. eq 5.1; here U''_m is the second derivative of $U(h)$ at the point of its maximum (at $h = h_m$).

5.2. Expression for the Interaction Energy. To obtain quantitative results from eq 5.5, one has to estimate the interaction energy $U(h)$. First of all, we can adapt Derjaguin's approximation[34,35] to the case of a cylinder of length L parallel to a planar phase boundary (Figure 3a):

$$U = L\int_{-a}^{+a} f(\tilde{h}(x))\,\mathrm{d}x \tag{5.6}$$

Here a is the radius of the cross section of the cylindrical micelle. The xy-plane coincides with the planar phase boundary, the x-axis being oriented perpendicularly to the cylinder axis; $f(\tilde{h})$ is the interaction free energy/unit area of a plane-parallel film of thickness $\tilde{h}$. The shape of the gap in the contact zone plane−cylinder can be approximated with a parabola

$$\tilde{h}(x) = h + x^2/(2a) \tag{5.7}$$

Next, we use eq 5.7 to change the integration variable in eq 5.6:

$$U(h) = (2a)^{1/2}L\int_h^\infty f(\tilde{h})\frac{\mathrm{d}\tilde{h}}{(\tilde{h}-h)^{1/2}} = (8a)^{1/2}L\int_h^\infty \Pi(\tilde{h})(\tilde{h}-h)^{1/2}\,\mathrm{d}\tilde{h} \tag{5.8}$$

At the last step we have applied integration by parts and the identity $\Pi(\tilde{h}) = -\partial f/\partial\tilde{h}$, where Π is the disjoining pressure.[34,35]

5.3. Modeling the Surface Forces. Our purpose here is to illustrate how the barrier to adsorption can be estimated using the simplest possible model. To get numerical results we have to specify the dependence $\Pi(h)$. As already mentioned, close to the cloud point the steric repulsion between the ethoxy chains of the nonionic surfactant is converted into attraction. (The same attraction is related to the appearance of bigger and bigger micelles when approaching the cloud point from below.) In other words, the water becomes a poor solvent for the poly(ethylene oxide). Under such conditions, the ethoxy brushes of the surfactant adsorption monolayers are more compact and dense, which decreases the steric (osmotic, overlap) repulsion between such brushes at two approaching interfaces.[25,36] Other types of surface forces, which are expected to be operative, are the van der Waals attraction, the electrostatic (double layer) repulsion, and the short-range hydrophobic attraction.[25] For the sake of a first estimate, below we follow the DLVO model, attributing the attraction to the van der Waals force and the repulsion to the double layer (electrostatic) force. In other words, for the specific experimental conditions (water, a poor solvent) we neglect the steric-overlap repulsion and the hydrophobic force. (The consequences of these approximations are discussed at the end of section 5.4.) This is equivalent to a treatment of the partially dehydrated ethoxy brushes as weakly hydrophobic oily layers. In such case, the surface electric charge can be due to binding of OH^- ions: note that the oil−water interface bears a considerable surface potential either in the presence or absence of adsorbed nonionic surfactants.[37,38] Thus, we arrive at the conventional DLVO expressions:[25,35,39]

$$\Pi(h) = \Pi_{vw}(h) + \Pi_{el}(h) \tag{5.9}$$

where

(31) Fuchs, N. A. *Z. Phys.* **1934**, *89*, 736.
(32) Derjaguin, B. V. *Theory of Stability of Colloids and Thin Liquid Films*; Plenum Press: New York, 1989.
(33) Leal, L. G. *Laminar Flow and Convective Transport Processes*; Butterworth-Heinemann: Boston, MA, 1992.
(34) Derjaguin, B. V. *Kolloid-Z.* **1934**, *69*, 155.
(35) Derjaguin, B. V.; Churaev, N. V.; Muller, V. M. *Surface Forces*; Plenum Press: New York, 1987.
(36) Russel, W. B.; Saville, D. A.; Schowalter, W. R. *Colloidal Dispersions*; Cambridge University Press: Cambridge, U.K., 1989.
(37) Velev, O. D.; Gurkov, T. G.; Alargova, R.; Marinova, K.; Ivanov, I. B.; Borwankar, R. P. *Proceedings of the First World Congress on Emulsion*; EDS Editeur: Paris, 1993; Vol. 1, Contribution No. 1.22.130.
(38) Marinova, K. G.; Alargova, R. G.; Denkov, N. D.; Velev, O. D.; Petsev, D. N.; Ivanov, I. B.; Borwankar, R. P. *Langmuir* **1996**, *12*, 2045.

$$\Pi_{vw}(h) = -\frac{A_H}{6\pi h^3} \quad \Pi_{el}(h) = B\exp(-\kappa h) \quad (5.10)$$

$$B \equiv 64IkT\gamma^2 \quad \kappa^2 = (8\pi e^2 I)/(\epsilon kT) \quad (5.11)$$

A_H is the Hamaker constant, I is the ionic strength of the solution, $\gamma = \tanh(e\psi_s/4kT)$, ψ_s is the surface electric potential, and ϵ is the dielectric constant of the medium (water). Substituting eqs 5.9−5.11 into eq 5.8 and integrating, we obtain

$$U(h)/(kT) = -\tilde{A}(\kappa h)^{-3/2} + \tilde{B}\exp(-\kappa h) \quad (5.12)$$

where $\tilde{A}$ and $\tilde{B}$ are dimensionless parameters independent of h:

$$\tilde{A} = \frac{A_H\kappa^{3/2}(2a)^{1/2}L}{24kT} \quad \tilde{B} = 64(2\pi a)^{1/2}\kappa^{-3/2}LI\gamma^2 \quad (5.13)$$

Using the condition that the energy $U(h)$ has a maximum (Figure 7), i.e., $dU/dh = 0$ at $h = h_m$, from eq 5.12 we obtain

$$\tilde{A} = \frac{2}{3}\tilde{B}y^{5/2}e^{-y} \quad y \equiv \kappa h_m \quad (5.14)$$

With the help of eqs 5.4, 5.12, and 5.14, one can bring the expression for the rate constant, eq 5.5, in a dimensionless form, which is convenient for computations:

$$\tilde{k}_{1,a} = (-\tilde{U}''_m)^{1/2}\left(\frac{y}{\tilde{a}}\right)^{3/2}\exp(-\tilde{E}_a) \quad (5.15)$$

where

$$\tilde{E}_a = (1 - 2y/3)\tilde{B}\exp(-y) \quad (5.16)$$

$$-U''_m = (2.5 - y)\frac{\tilde{B}}{y}\exp(-y) \quad (5.17)$$

The dimensionless parameters are defined as follows:

$$\tilde{E}_a = \frac{E_a}{kT} \quad \tilde{a} = \pi\kappa a \quad \tilde{k}_{1,a} = \frac{6\eta L}{\kappa kT}k_{1,a} \quad (5.18)$$

5.4. Discussion. If $k_{1,a}$ is obtained experimentally, from eqs 5.15 and 5.16 (along with 5.17) one can determine the two unknown variables $\tilde{E}_a$ and y, and thus, to find the height and position of the barrier, supposedly the values of all other parameters are known.

For example, in section 3.3 we found $k_{1,a} = 336$ nm/s for the system 12 mM $C_{12}E_5$ + 0.1 wt % SL61 + 0.01 M NaCl. Hence, we have $I = 0.01$ M and $\kappa^{-1} = 3.04$ nm; from Table 1 in ref 21 we take the values $a = 2.8$ nm and $L = 2pa = 134.4$ nm at $T = 300$ K. We have to assign value to one additional parameter, either to the Hamaker constant A_H or to the surface potential ψ_s (if one of them is given, the other one can be calculated). Since the computations are less sensitive to the surface potential, we choose to assign a value to ψ_s and to predict A_H. We take a reasonable value for a partially hydrophobic surface in water (e.g., carbon particles in water[40]), $|\psi_s| = 15$ mV, which yields $\tilde{B} = 24.32$.

With these parameter values we solve eq 5.15 (along with eqs 5.16 and 5.17) and obtain $y = 0.599$. Furthermore, by using eqs 5.13, 5.14, and 5.16, we find that the height of the barrier is $E_a = 8.0kT$, its position is at $h_m = 1.8$ nm, and the Hamaker constant (characterizing the attractive surface force) is $A_H = 4.1 \times 10^{-21}$ J. Figure 7 illustrates the respective dependence $U(h)$ calculated by means of eq 5.12. The obtained parameter values seem quite reasonable having in mind the approximations used (the Derjaguin approximation, the steepest descent method, neglecting the steric and hydrophobic surface forces, and assumptions for monodisperse rodlike micelles and for micelle axis parallel to the interface). In particular, if the hydrophobic attraction were significant, we would obtain a nonrealistically high value of A_H, which is not the case. It turns out that the hydrophobic attraction is counterbalanced by the steric-overlap repulsion, or both are negligible, so that the conventional DLVO theory provides a reasonable description.

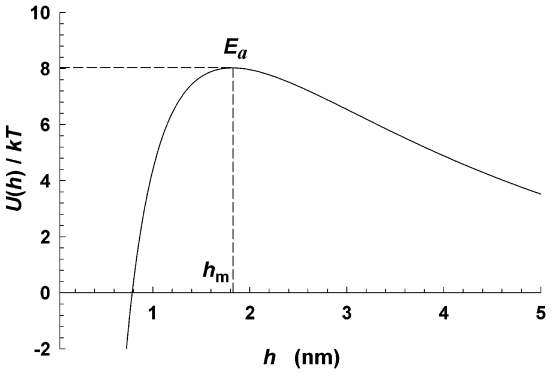

Figure 7. Plot of the interaction energy, U, vs the surface-to-surface distance, h, between a micelle and the interface (Figure 3a). The curve is drawn using eq 5.12 and corresponds to parameter values $\psi_s = -15$ mV and $A_H = 4.1 \times 10^{-21}$ J (see the text for details).

The rate of micelle adsorption (and the overall rate of solubilization) is most sensitive to the height of the barrier, E_a. Equations 5.13 and 5.16 show that

$$E_a \propto L \quad (5.19)$$

(at fixed other parameters). Hence, one of the reasons the copolymer SL61 acts as a promoter of solubilization is that it reduces the length of the micelles (without increasing their surface electric charge), and thus lowers the barrier to their adsorption at the oil−water interface. This could also explain, at least in part, the effect of hydrophilic alcohols on the solubilization by nonionic surfactant micelles: it has been found[13,15] that the addition of such alcohols decreases the micelle size and accelerates the process of solubilization.

Finally, it is worthwhile noting that, in our kinetic model, based on mass balances, we have used the mean mass values of the micelle diffusivity, D_1, and the bulk concentration, c_{10}, determined by light scattering as explained in part 1.[21] In other words, we have approximately considered the rodlike micelles as monodisperse aggregates characterized by the respective mean mass values. The real micelle size distribution is known to be relatively polydisperse.[25−27,41] A further development of the proposed model could take into account the effect of polydispersity of the elongated micelles.

6. Summary and Conclusions

On the basis of recent experimental results,[21,22] in this paper we propose a theoretical model of solubilization of

(39) Kralchevsky, P. A.; Nagayama, K. *Particles at Fluid Interfaces and Membranes*; Elsevier: Amsterdam, 2001.

(40) Krishnakumar, S.; Somasundaran, P. *Colloids Surf., A* **1996**, *117*, 227.

(41) Missel, P. J.; Mazer, N. A.; Benedek, G. B.; Young, C. Y.; Carey, M. C. *J. Phys. Chem.* **1980**, *84*, 1044.

oil drops in micellar surfactant solutions. We consider oils that are practically insoluble in pure water, like triolein and other triglycerides. The micelles, which are capable to solubilize such oils, are long rodlike aggregates, composed of nonionic surfactant and triblock copolymers. The swollen micelles, formed after solubilization, are smaller than the empty ones.[21]

The model describes the elementary act of solubilization as a sequence of three steps (Figure 3): (a) adsorption of an empty micelle at the oil−water interface; (b) surface reaction, described by eq 3.1, where the empty micelle takes oil and splits into several swollen micelles; (c) desorption of the formed swollen micelles.

In conformity with our experiments,[22] we assume that the micelle transport in the solution occurs in a mixed, barrier-diffusion regime. A differential equation is obtained, eq 3.10, which describes the diminishing of the oil-drop radius in the course of solubilization, $R = R(t)$. For micelle adsorption in the Henry regime (low surface coverage), we derived a convenient explicit formula for $R(t)$; see eq 3.18. The latter can be used to fit experimental data and to determine the two parameters of the model, α and β; see eqs 3.16 and 3.17. From the values of α and β one can calculate the number of oil molecules solubilized in a swollen micelle, n_s, and the solubilization kinetic parameter, χ; see eq 3.20.

The parameter values, determined from the fit of the data in Figure 5, imply that the process of desorption of swollen micelles from the oil−water interface (Figure 3c) is much slower than the uptake of oil (Figure 3b), that is, $k_{1,d} \ll k_s$, at least for the considered specific system. In such a case, eq 3.13 implies $\chi \approx k_{1,a}$; that is, the adsorption step (Figure 3a) becomes the rate-controlling one. In section 5, from the experimental rate constant of adsorption we estimate the respective kinetic barrier to adsorption, E_a, taking into account the action of surface forces and the hydrodynamic resistance; see eqs 5.5 and 5.16 and Figure 7.

The theoretical analysis shows that the block copolymer SL61 promotes the solubilization of triglycerides mostly by decreasing the length L of the mixed surfactant−copolymer rodlike micelles, which leads to a lowering the kinetic barrier E_a to micelle adsorption; see eq 5.19.

The obtained theoretical expressions are applied in the next part of this study[22] to interpret a set of experimental data for solubilization of Triolein in micellar solutions of $C_{12}E_5$ and $C_{12}E_6$ at various concentrations of added copolymer SL61.

Acknowledgment. The support by Colgate-Palmolive is gratefully acknowledged. The authors are indebted to Prof. Krassimir Danov for his consultation concerning the hydrodynamic resistance factor.

LA020366K